

Long-lived Sterile Neutrinos at Belle II in Effective Field Theory

Guanghai Zhou,^{a,b} Julian Y. Günther,^c Zeren Simon Wang,^{d,e} Jordy de Vries,^{a,b} and Herbi K. Dreiner^c

^a*Institute for Theoretical Physics Amsterdam and Delta Institute for Theoretical Physics, University of Amsterdam, Science Park 904, 1098 XH Amsterdam, The Netherlands*

^b*Nikhef, Theory Group, Science Park 105, 1098 XG, Amsterdam, The Netherlands*

^c*Bethe Center for Theoretical Physics & Physikalisches Institut der Universität Bonn, Nußallee 12, 53115 Bonn, Germany*

^d*Department of Physics, National Tsing Hua University, Hsinchu 300, Taiwan*

^e*Center for Theory and Computation, National Tsing Hua University, Hsinchu 300, Taiwan*

E-mail: g.zhou@uva.nl, guenther@physik.uni-bonn.de, wzs@mx.nthu.edu.tw, j.devries4@uva.nl, dreiner@uni-bonn.de

ABSTRACT: Large numbers of τ leptons are produced at Belle II. These could potentially decay into sterile neutrinos that, for the mass range under consideration, are typically long-lived, leading to displaced-vertex signatures. Here, we study a displaced-vertex search in the context of the sterile-neutrino-extended Standard Model Effective Field Theory. The production and decay of the sterile neutrinos can be realized via either the standard active-sterile neutrino mixing or higher-dimensional operators in the effective Lagrangian. We perform Monte-Carlo simulations to estimate the Belle II sensitivities to such interactions. We find that Belle II can probe non-renormalizable dimension-six operators involving a single sterile neutrino up to a few TeV in the new-physics scale.

Contents

1	Introduction	1
2	The νSMEFT Model	3
3	Theoretical Scenarios	5
3.1	The minimal Scenario	6
3.2	Scenarios from higher-dimensional Operators	7
4	Experiment and Simulation	10
5	Numerical Results	12
6	Conclusions	15
A	Two-body Decay Processes with a Sterile Neutrino	16
A.1	Charged Currents	16
A.2	Neutral Currents	16
A.2.1	The Two-body Decay of the Sterile Neutrino in the Minimal Model	16
A.2.2	The Two-body Decay of the Sterile Neutrino via higher-dimensional Operators	17
B	Three-body Decays	18

1 Introduction

The observation of neutrino oscillations has established active neutrinos as massive particles [1], inconsistent with the prediction of the Standard Model (SM) of particle physics. The $SU(2)_L \times U(1)_Y$ gauge invariance and the absence of right-handed neutrinos forbid a renormalizable neutrino mass term. Thus, new physics (NP) is required to explain the neutrino masses. A minimal solution is to add right-handed gauge-singlet sterile neutrinos to the SM [2–6], which can interact with the SM particles via Yukawa interactions, generating Dirac neutrino masses after electroweak (EW) symmetry breaking. Without violating Lorentz symmetry or SM gauge symmetries, the sterile neutrinos can also have a Majorana mass term, which violates lepton number by two units and can result in lepton-number-violating processes such as neutrinoless double beta decay [7]. With a so-called seesaw mechanism, tiny active neutrino masses, in agreement with observations [1, 8, 9], arise from $\mathcal{O}(1)$ Yukawa couplings and sterile neutrino masses of GUT (Grand Unified Theory) scale $\sim 10^{15}$ GeV. But much smaller sterile masses are equally fine, just requiring smaller Yukawa couplings.

Besides being a minimal solution, sterile neutrinos are also predicted in a wide range of beyond-the-Standard-Model (BSM) models, such as GUTs [10], Z' models [11, 12], left-right symmetric models [13–16], and leptoquark models [17]. Beyond the sterile neutrinos, these models predict new particles that are often heavy compared to the EW scale. One useful and systematic way to describe such new physics is to apply effective field theory (EFT), where the heavy degrees of freedom are integrated out, leading to non-renormalizable operators in the Lagrangian. These are gauge invariant and consist of light fields only. The EFT that describes the interaction of the sterile neutrinos with SM particles is known as ν SMEFT [18–23], which we apply in this work.

If the sterile neutrinos are light, *e.g.* at the GeV scale, and their mixings with the active neutrinos are tiny and/or the NP scale is heavy, their decay rates are suppressed and the sterile neutrinos become long-lived. If such a neutrino is produced at an experiment it can travel a macroscopic distance, before decaying into, hopefully, visible final states. Searches for such sterile neutrinos have been both performed and proposed at various experimental facilities. Past experiments including Belle [24], PS191 [25, 26], L3 [27], T2K [28], CHARM [29, 30], NuTeV [31], NA3 [32], BEBC [33], and DELPHI [34] have attained constraints for sterile neutrino masses below the W -boson mass. More recently, LHCb [35, 36], and CMS [37, 38] have also searched for such exotics. In addition, ATLAS at the LHC has searched for sterile neutrinos which mix with either ν_e or ν_μ [39, 40]. Furthermore, a number of far-detector experiments such as FASER [41] and MATHUSLA [42] have been proposed to be operated in the vicinity of various LHC interaction points (IPs). These are planned as dedicated detectors to hunt for long-lived particles (LLPs) in general¹, and their sensitivities to long-lived sterile neutrinos have been studied extensively [11, 46–51]. Besides, excellent sensitivities to such scenarios are also expected at future electron-positron and electron-proton colliders such as the CEPC, FCC-ee, LHeC, and FCC-he [52–58]. Finally, B -factories such as the ongoing Belle II experiment, colliding electron and positron beams at relatively low center-of-mass (CM) energies, could also look for sterile neutrinos lighter than B -mesons [24, 59–61].

In this work, we focus on the B -factory experiment Belle II, which is in operation in Japan. At Belle II, an electron beam of energy 7 GeV collides with a positron beam of energy 4 GeV, reaching the CM energy 10.58 GeV, *i.e.* at the $\Upsilon(4S)$ resonance. With a projected integrated luminosity of 50 ab^{-1} , this results in a very large number of $B\bar{B}$ events. Besides, Belle II is estimated to generate a large number of τ -pair production events, allowing for the study of rare τ decays to an unprecedented precision. This includes studying lepton flavor violation [62–66] and LLPs [61, 64, 67–76]. In particular, Ref. [61] has studied the Belle II exclusion limits for long-lived sterile neutrinos which mix dominantly with ν_τ , by considering τ decays. Here, we propose a displaced-vertex search strategy similar to that discussed in Ref. [61], reproducing the minimal-scenario results, as well as extending the physics coverage to several scenarios in the ν SMEFT, where one single EFT operator can lead to both production and decay of the sterile neutrinos.

The paper is organized as follows. We first introduce the ν SMEFT theoretical framework in Sec. 2. We discuss both the minimal scenario and a series of EFT scenarios in

¹See Refs. [42–45] for recent reviews of LLP models and searches.

Sec. 3, for all of which we perform numerical studies. The Belle II experiment is detailed in Sec. 4 together with a description of our search strategy. The numerical results are presented in Sec. 5, and we conclude the paper in Sec. 6. Appendices A and B detail the computation of two- and three-body decay rates of the sterile neutrinos.

2 The ν SMEFT Model

For simplicity, we consider the SM extended by only one right-handed gauge-singlet neutrino ν_R . The SM Lagrangian is then augmented by new renormalizable terms: a Majorana mass term and a Yukawa term

$$\mathcal{L} = \mathcal{L}_{\text{SM}} - \left[\frac{1}{2} \bar{\nu}_R^c \bar{M}_R \nu_R + \bar{L} \tilde{H} Y_\nu \nu_R + \text{h.c.} \right], \quad (2.1)$$

where \mathcal{L}_{SM} denotes the SM Lagrangian, $L = (\nu_L, e_L)^T$ is the lepton doublet, H is the Higgs doublet, and $\tilde{H} = i\tau_2 H^*$. In the unitary gauge,

$$H = \frac{v}{\sqrt{2}} \begin{pmatrix} 0 \\ 1 + \frac{h}{v} \end{pmatrix}, \quad (2.2)$$

where $v = 246$ GeV is the Higgs vacuum expectation value and h is the SM Higgs scalar. \bar{M}_R is the Majorana mass for the sterile neutrino and Y_ν is a 3×1 matrix of Yukawa couplings. We work in the basis where the charged leptons $e_{L,R}^i$, the quarks $u_{L,R}^i$, and d_L^i ($i = 1, 2, 3$) are in their mass eigenstates. For d_L^i we have $d_L^i = V^{ij} d_L^{j, \text{mass}}$, where V is the CKM matrix and $d_L^{j, \text{mass}}$ denotes the left-handed down-type quarks in the mass basis. ν_R^c is the charge conjugate field of ν_R with $\nu_R^c = C \bar{\nu}_R^T$ and $C = -i\gamma^2 \gamma^0$, in four-component fermion notation.

Additional new physics at a higher energy scale can lead to higher-dimensional operators involving the ν_R above the electroweak scale. The possible dimension-5 operators are

$$\mathcal{L}_{\nu_L}^{(5)} = \epsilon_{kl} \epsilon_{mn} (L_k^T C_L^{(5)} C L_m) H_l H_n, \quad \mathcal{L}_{\nu_R}^{(5)} = -\bar{\nu}_R^c C_R^{(5)} \nu_R H^\dagger H. \quad (2.3)$$

Here, C is the charge conjugation matrix, as before. $C_L^{(5)}$ and $C_R^{(5)}$ are arbitrary coefficients with mass dimension -1. The first term is also known as the Weinberg operator. Both terms contribute to the Majorana masses for the active and sterile neutrinos, respectively, after electroweak symmetry breaking (EWSB). Thus, at low energy, these terms only lead to a shift in the free parameter \bar{M}_R , and are not relevant for our analysis.

Here, we are interested in operators with just one sterile neutrino up to dimension six [20, 77]. We list the relevant ones in Table 1². They are organized in four classes according to powers of the fermion (ψ) and Higgs fields (H): $\psi^2 H^3$, $\psi^2 H^2 D$, $\psi^2 H F$, ψ^4 , where D denotes a covariant derivative and F is a gauge field strength tensor. We use C_I to denote the Wilson coefficients of operator \mathcal{O}_I . Furthermore, each carries two or four generation indices for the quarks and leptons.

²In principle, there are also dimension-six operators with two or four sterile neutrinos. See Ref. [20] for a summary. In particular, operators with a pair of sterile neutrinos can enhance the production of the sterile neutrinos, which then may dominantly decay via mixing with the SM active neutrinos. See Ref. [48] for a recent study on this scenario at the LHC.

Class 1	$\psi^2 H^3$	Class 4	ψ^4
$\mathcal{O}_{L\nu H}$	$(\bar{L}\nu_R)\tilde{H}(H^\dagger H)$	\mathcal{O}_{duve}	$(\bar{d}_R\gamma^\mu u_R)(\bar{\nu}_R\gamma_\mu e)$
Class 2	$\psi^2 H^2 D$	\mathcal{O}_{QuvL}	$(\bar{Q}u_R)(\bar{\nu}_R L)$
$\mathcal{O}_{H\nu e}$	$(\bar{\nu}_R\gamma^\mu e_R)(\tilde{H}^\dagger iD_\mu H)$	$\mathcal{O}_{L\nu Qd}$	$(\bar{L}\nu_R)\epsilon(\bar{Q}d_R)$
Class 3	$\psi^2 HF$	$\mathcal{O}_{LdQ\nu}$	$(\bar{L}d_R)\epsilon(\bar{Q}\nu_R)$
$\mathcal{O}_{\nu W}$	$(\bar{L}\sigma_{\mu\nu}\nu_R)\tau^I\tilde{H}W^{I\mu\nu}$	$\mathcal{O}_{L\nu Le}$	$(\bar{L}\nu_R)\epsilon(\bar{L}e_R)$
$\mathcal{O}_{\nu B}$	$(\bar{L}\sigma_{\mu\nu}\nu_R)\tilde{H}B^{\mu\nu}$		

Table 1. Dimension-six operators involving one sterile neutrino field ν_R . Each fermion field has a generation index, except ν_R . When needed, we shall attach these indices to the operator symbol. Thus, $\mathcal{O}_{duve}^{21\nu R3}$ refers to the operator $(\bar{s}\gamma^\mu u)(\bar{\nu}_R\gamma_\mu \tau)$.

After EWSB, the operator $\mathcal{O}_{L\nu H}$ contributes to the Dirac mass of the neutrino. This can be absorbed in a re-definition of Y_ν and will therefore not be considered for the rest of the paper. $\mathcal{O}_{\nu W}$ and $\mathcal{O}_{\nu B}$ induce higher-dimensional operators with much smaller coefficients compared to the other operators [7, 51] listed in Table 1 and are strictly constrained by neutrino dipole moments [78, 79], so will not be considered further. The remaining interactions are gauge invariant under $SU(3)_C \times U(1)_{EM}$ and can be written as

$$\begin{aligned} \mathcal{L} = \mathcal{L}_{SM} - & \left[\frac{1}{2}\bar{\nu}_L^c M_L \nu_L + \frac{1}{2}\bar{\nu}_R^c M_R \nu_R + \bar{\nu}_L M_D \nu_R + \text{h.c.} \right] \\ & + \mathcal{L}_{CC}^{(6)} + \mathcal{L}_{NC}^{(6)}, \end{aligned} \quad (2.4)$$

where \mathcal{L}_{SM} denotes the renormalizable Lagrangian involving only light SM fields after EWSB. M_L is a 3×3 Majorana mass matrix, M_R is a Majorana mass parameter, and M_D is a 3×1 Dirac mass matrix. $\mathcal{L}_{CC}^{(6)}$ contains charged-current interactions and is given by

$$\begin{aligned} \mathcal{L}_{CC}^{(6)} = \frac{2G_F}{\sqrt{2}} & \left\{ \bar{u}_L^i \gamma^\mu d_L^j \left[\bar{e}_L^k \gamma_\mu c_{VLL,ijkl}^{CC} \nu_L^l + \bar{e}_R^k \gamma_\mu c_{VLR,ijk}^{CC1} \nu_R \right] + \bar{u}_R^i \gamma^\mu d_R^j \bar{e}_R^k \gamma_\mu c_{VRR,ijk}^{CC} \nu_R \right. \\ & + \bar{u}_L^i d_R^j \bar{e}_L^k c_{SRR,ijk}^{CC1} \nu_R + \bar{u}_R^i d_L^j \bar{e}_L^k c_{SLR,ijk}^{CC} \nu_R + \bar{u}_L^i \sigma^{\mu\nu} d_R^j \bar{e}_L^k \sigma_{\mu\nu} c_{T,ijk}^{CC} \nu_R \\ & \left. + \bar{e}_L^i c_{SRR,ijk}^{CC2} \nu_R \bar{\nu}_L^j e_R^k + \bar{\nu}_L^i \gamma^\mu e_L^j \bar{e}_R^k \gamma_\mu c_{VLR,ijk}^{CC2} \nu_R \right\} + \text{h.c.} - \frac{4G_F}{\sqrt{2}} \bar{\nu}_L^i \gamma^\mu e_L^i \bar{e}_L^j \gamma_\mu \nu_L^j, \end{aligned} \quad (2.5)$$

where we include terms involving only active neutrinos ν_L from the SM weak interaction and i, j, k, l are the flavor indices of the quarks and leptons, and a summation over them is

implied. Similarly, for the neutral-current interactions $\mathcal{L}_{NC}^{(6)}$, we have

$$\begin{aligned}
\mathcal{L}_{NC}^{(6)} = & \frac{-4G_F}{\sqrt{2}} \bar{\nu}_L^i \gamma^\mu \nu_L^i \left\{ \bar{e}_L^j \gamma_\mu \left(-\frac{1}{2} + \sin^2 \theta_W \right) e_L^j + \bar{e}_R^j \gamma_\mu (\sin^2 \theta_W) e_R^j \right. \\
& + \bar{u}_L^j \gamma^\mu \left(\frac{1}{2} - \frac{2}{3} \sin^2 \theta_W \right) u_L^j + \bar{u}_R^j \gamma_\mu \left(-\frac{2}{3} \sin^2 \theta_W \right) u_R^j \\
& + \bar{d}_L^j \gamma^\mu \left(-\frac{1}{2} + \frac{1}{3} \sin^2 \theta_W \right) d_L^j + \bar{d}_R^j \gamma_\mu \left(\frac{1}{3} \sin^2 \theta_W \right) d_R^j + \frac{1}{4} (2 - \delta_{ij}) \bar{\nu}_L^j \gamma^\mu \nu_L^j \left. \right\} \\
& + \frac{2G_F}{\sqrt{2}} \left\{ \bar{u}_R^i u_L^j \bar{\nu}_L^k c_{SLR,ijk}^{NC} \nu_R + \bar{d}_L^i d_R^j \bar{\nu}_L^k c_{SRR,ijk}^{NC1} \nu_R + \bar{\nu}_L^i c_{SRR,ijk}^{NC2} \nu_R \bar{e}_L^j e_R^k \right. \\
& \left. + \bar{d}_L^i \sigma^{\mu\nu} d_R^j \bar{\nu}_L^k \sigma_{\mu\nu} c_{T,ijk}^{NC} \nu_R + \text{h.c.} \right\}, \tag{2.6}
\end{aligned}$$

where θ_W is the electroweak mixing angle. Here, we give the matching relations [7]. For the mass terms we find

$$M_L = -v^2 C_L^{(5)}, \quad M_R = \bar{M}_R + v^2 C_R^{(5)}, \quad M_D = \frac{v}{\sqrt{2}} \left[Y_\nu - \frac{v^2}{2} C_{L\nu H} \right]. \tag{2.7}$$

The matching relations for the charged-current operators are

$$\begin{aligned}
c_{VLL,ijk}^{CC} &= -2V_{ij} \delta_{kl}, & c_{VLR,ijk}^{CC1} &= [-v^2 C_{H\nu e,k}]^\dagger V_{ij}, \\
c_{VLR,ijk}^{CC2} &= [-v^2 C_{H\nu e,k}]^\dagger \delta_{ij}, & c_{VRR,ijk}^{CC} &= v^2 (C_{d\nu e,jik})^\dagger, \\
c_{SRR,ijk}^{CC1} &= -v^2 C_{L\nu Qd,kij} + \frac{v^2}{2} C_{LdQ\nu,kji}, & c_{SLR,ijk}^{CC} &= v^2 (C_{Q\nu L,lik})^\dagger V_{lj}, \\
c_{T,ijk}^{CC} &= \frac{v^2}{8} C_{LdQ\nu,kji}, & c_{SRR,ijk}^{CC2} &= -v^2 C_{L\nu Le,ijk}, \tag{2.8}
\end{aligned}$$

with V the CKM matrix. For the neutral-current operators we find

$$\begin{aligned}
c_{SLR,ijk}^{NC} &= v^2 (C_{Q\nu L,jik})^\dagger, & c_{SRR,ijk}^{NC1} &= v^2 C_{L\nu Qd,klj} V_{li}^* - \frac{v^2}{2} C_{LdQ\nu,kjl} V_{li}^*, \\
c_{SRR,ijk}^{NC2} &= v^2 C_{L\nu Le,ijk}, & c_{T,ijk}^{NC} &= -\frac{v^2}{8} C_{LdQ\nu,kjl} V_{li}^*, \tag{2.9}
\end{aligned}$$

where V_{li}^* is the charge conjugate of V_{li} .

The renormalization group equations for these ν SMEFT operators arising from one-loop QCD effects have been discussed in Ref. [7]. The overall effect there was found to be minor and we neglect the effect here.

3 Theoretical Scenarios

In this section, we study various possible channels for the production and decay of sterile neutrinos at Belle II. We extend the SM by adding a Majorana sterile neutrino ν_R , as well as the non-renormalizable interactions given in Table 1. The sterile neutrino is produced by the decay of τ leptons either from the mixing between active and sterile neutrinos, or from the new higher-dimensional operators.

$\tau^- \rightarrow \nu_R (\bar{\nu}_R) + X_1$ & $\nu_R \rightarrow X_2$	X_1	X_2
Minimal scenario	$\pi^-, \rho^-, K^-, K^{*-},$ $e^- + \bar{\nu}_e, \mu^- + \bar{\nu}_\mu$	$(\pi^0, \rho^0, \eta, \eta', \omega, \phi,$ $\bar{\nu}_e + \nu_e, \bar{\nu}_\mu + \nu_\mu, \bar{\nu}_\tau + \nu_\tau,$ $e^- + e^+, \mu^- + \mu^+) + \nu_\tau$
Scenario $\mathcal{O}_{LvQd}^{3\nu_R 11}$	π^-	$(\pi^0, \eta, \eta', K^0) + \nu_\tau$
Scenario $\mathcal{O}_{QuvL}^{11\nu_R 3}$	π^-, K^-	$(\pi^0, \eta, \eta') + \nu_\tau$
Scenario $\mathcal{O}_{H\nu e}^{\nu_R 1}$	$e^- + \nu_\tau (+\bar{\nu}_R)$	$(\pi^+, \rho^+, K^+, K^{*+},$ $e^+ + \nu_e, \mu^+ + \nu_\mu) + e^-$
Scenario $\mathcal{O}_{duve}^{11\nu_R 3}$ & $\mathcal{O}_{duve}^{11\nu_R 1}$	π^-, ρ^-	$(\pi^+, \rho^+) + e^-$
Scenario $\mathcal{O}_{LvLe}^{1\nu_R 31}$	$e^- + \bar{\nu}_e$	$e^- + \nu_\tau + e^+$
Scenario $\mathcal{O}_{LdQ\nu}^{311\nu_R}$	π^-, ρ^-	$(\pi^0, \rho^0, \omega, \eta, \eta', K^0, K^{*0}) + \nu_\tau$

Table 2. All possible production, X_1 , and decay, X_2 , modes of a sterile neutrino ν_R at Belle II. The charge conjugate modes are implied.

3.1 The minimal Scenario

We first consider the minimal model, where a sterile neutrino interacts with SM particles only through the mixing between the active tau-neutrino ν_τ and the sterile neutrino. The Lagrangian is obtained by setting all the Wilson coefficients c^{CC} and c^{NC} except c_{VLL}^{CC} in Eqs. (2.5) and (2.6) to zero. The active neutrinos ν_α can be expressed in terms of neutrino mass eigenstates ν_i

$$\nu_\alpha = U_{\alpha i} \nu_i, \quad (3.1)$$

where $\alpha = e, \mu, \tau$ and $i = 1, 2, 3, 4$. We only consider the mixing between ν_τ and the sterile neutrino proportional to $U_{\tau 4}$ as the mixing matrix elements U_{e4} and $U_{\mu 4}$ are severely constrained from other observables, see *e.g.* Refs. [51, 80]. We neglect the masses of the active neutrinos. As a result of the small mixing $U_{\tau 4}$, ν_R is approximately equivalent to ν_4 , and we hence refer to both of them as the sterile neutrino. The production and decay rates depend on two independent parameters, the mixing matrix element $U_{\tau 4}$ and the mass of the sterile neutrino m_N . We list all the possible resulting production and decay channels in the minimal scenario in the second row of Table 2. For instance, with $X_1 = K^-$ and $X_2 = e^- + e^+ + \nu_\tau$, we have the decay chain,

$$\tau^- \rightarrow \nu_R + K^-, \quad \text{followed by,} \quad \nu_R \rightarrow e^- + e^+ + \nu_\tau. \quad (3.2)$$

The branching ratios of the production and decay channels are displayed in Fig. 1 and Fig. 2, as functions of m_N . As explained in Sec. 4, we do not consider all the decay channels of ν_R as visible. Therefore, in Fig. 2 only the visible channels are shown. The resulting proper decay length of the sterile neutrino times $|U_{\tau 4}|^2$ is presented in Fig. 3. For a discussion of the explicit expression of the decay rates, we refer to the Appendices A and B.

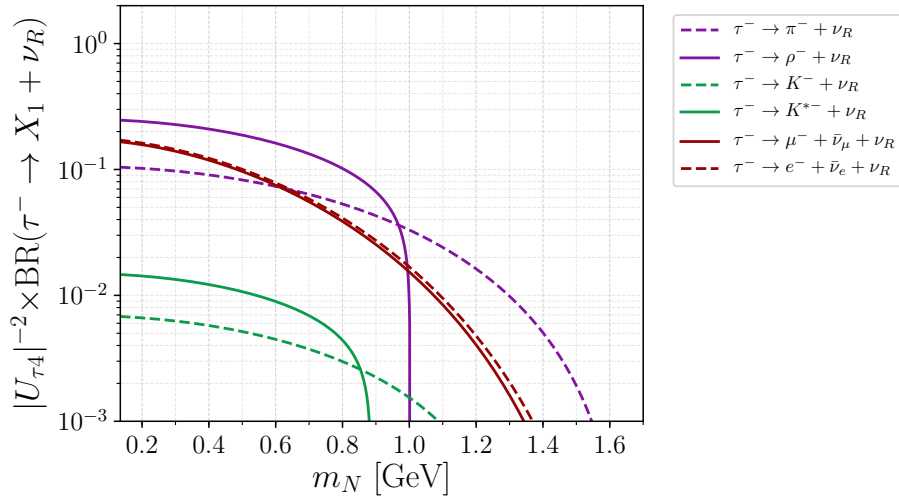


Figure 1. Tau decay branching ratios into a sterile neutrino in the minimal scenario.

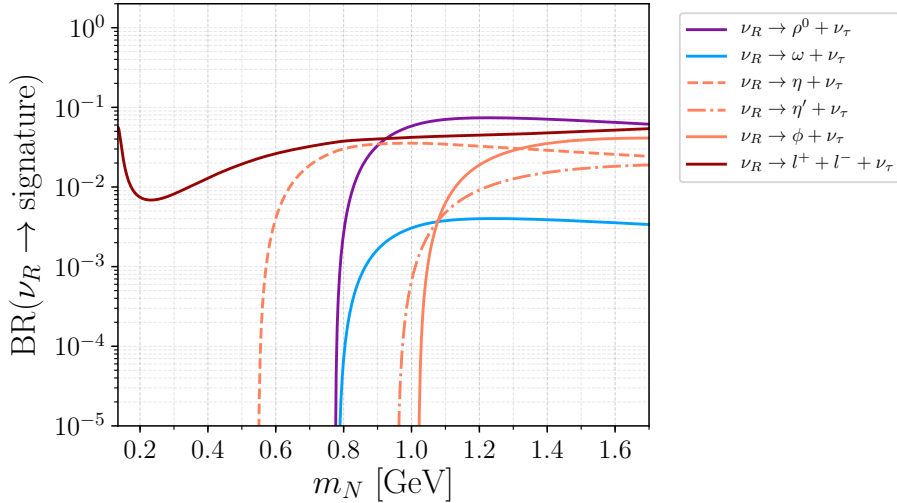


Figure 2. Branching ratios of visible decay modes in the minimal scenario.

3.2 Scenarios from higher-dimensional Operators

We now discuss scenarios with the SM extended by one of the operators listed in Table 1, possibly with more than one index structure. Here, we assume the type-I seesaw relation, so that the effects from the active-sterile neutrino mixing are negligible³. We consider the following operators in turn: $\mathcal{O}_{Qu\nu L}$, $\mathcal{O}_{L\nu Qd}$, $\mathcal{O}_{L\nu Le}$, $\mathcal{O}_{H\nu e}$ and $\mathcal{O}_{LdQ\nu}$. While we refrain from specifying a UV-complete model, which is not necessary for the low-energy phenomenology we are after, it is worthwhile to mention that these operators can easily be obtained in leptoquark models ($\mathcal{O}_{LdQ\nu}$), models with Z' bosons ($\mathcal{O}_{Qu\nu L}$, $\mathcal{O}_{L\nu Qd}$, $\mathcal{O}_{L\nu Le}$), and left-right

³That is, here we practically neglect the interactions of the minimal model discussed in the previous subsection.

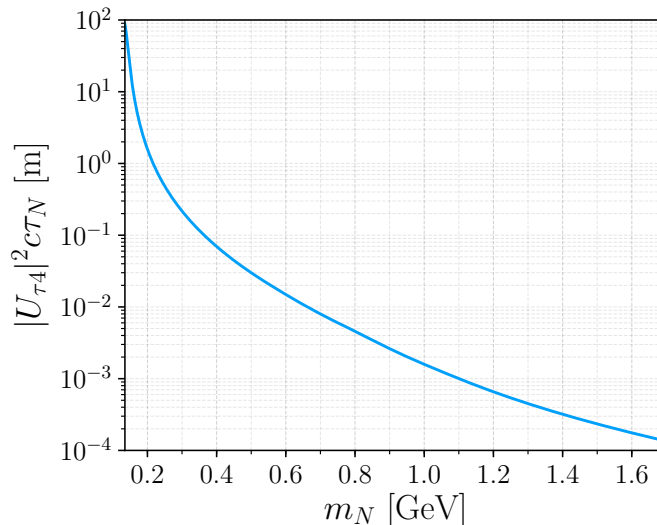


Figure 3. Proper decay length of the sterile neutrino times $|U_{\tau 4}|^2$ in the minimal scenario.

symmetric models ($\mathcal{O}_{H\nu e}$). We refer to Ref. [51] for a more detailed discussion.

The above operators are special in the sense that each of them can induce both the production and decay of sterile neutrinos by turning on only one flavor configuration. For example, with $\mathcal{O}_{Q\nu L}^{11\nu_R 3}$, we can have the decay chains,

$$\tau^- \rightarrow \nu_R + (\pi^-, K^-), \quad \nu_R \rightarrow \nu_\tau + (\pi^0, \eta, \eta'), \quad (3.3)$$

where the production of the sterile neutrino from τ^- decays can be associated with a K^- , because the left-handed down-type quarks d_L are not in their mass eigenstates. In choosing the flavor combinations, we focus exclusively on first-generation quarks.

For the operator $\mathcal{O}_{d\nu e}$, one single flavor setting cannot account for the production and decay of the sterile neutrino simultaneously. Hence, we choose $\mathcal{O}_{d\nu e}^{11\nu_R 3}$ for the production and $\mathcal{O}_{d\nu e}^{11\nu_R 1}$ for the decay, and assume that $C_{d\nu e}^{11\nu_R 3} = C_{d\nu e}^{11\nu_R 1}$. All the possible modes are listed in Table 2.

For each dimension-six operator in Table 1, we suppose their Wilson coefficients are given by $1/\Lambda^2$. The production and decay rates are thus proportional to $1/\Lambda^4$ and are functions of both m_N and Λ . In Fig. 4 and Fig. 5, we present respectively the τ decay branching ratios into a sterile neutrino plus anything and the proper decay lengths, $c\tau_N$, of the sterile neutrino, as functions of m_N , for a fixed value of $\Lambda = 1$ TeV. All the EFT scenarios summarized in Table 2 are included. Further, we show the branching ratios of the visible decay modes of the sterile neutrino in Fig. 6. The branching ratio of the signature decay mode in the scenario with the operator $\mathcal{O}_{L\nu Le}^{1\nu_R 31}$ is not included here, as it is 100%.

We note that in a recent paper [81], a phenomenological study on the EFT scenarios with the higher-dimensional operators listed in Table 2, except $\mathcal{O}_{H\nu e}$, has been performed for the LHC with a search strategy based on a displaced vertex, for $m_N \gtrsim 5$ GeV. In contrast, in this paper we focus on m_N below the τ -lepton mass.

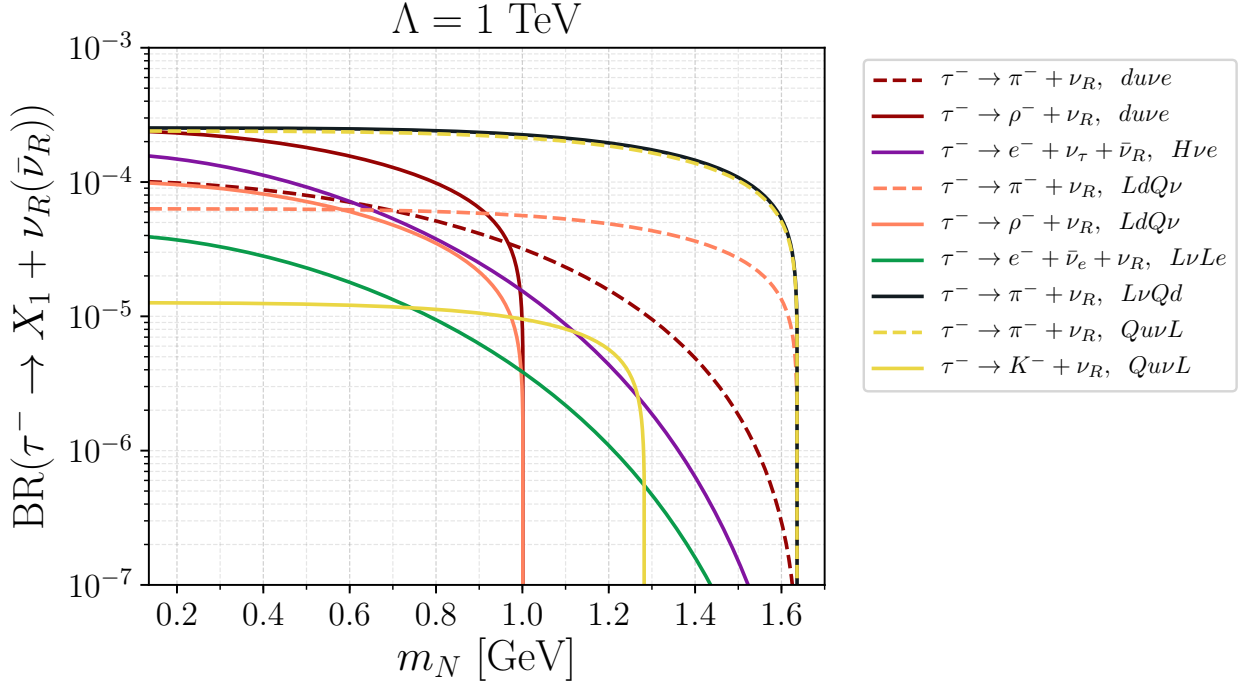


Figure 4. Tau decay branching ratios into a sterile neutrino for $\Lambda = 1 \text{ TeV}$.

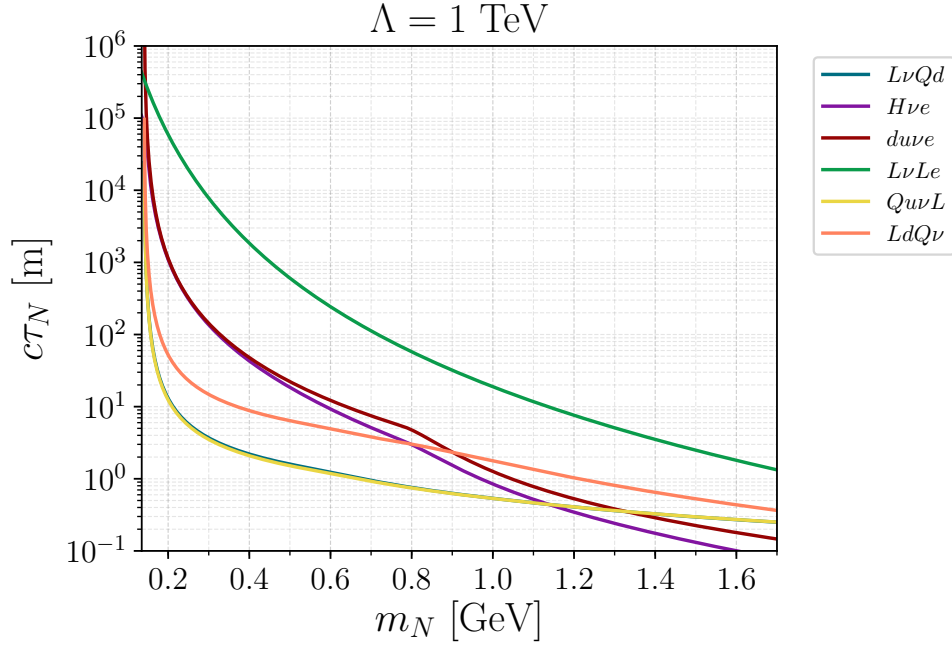


Figure 5. Proper decay lengths of the sterile neutrino in various EFT scenarios for $\Lambda = 1 \text{ TeV}$.

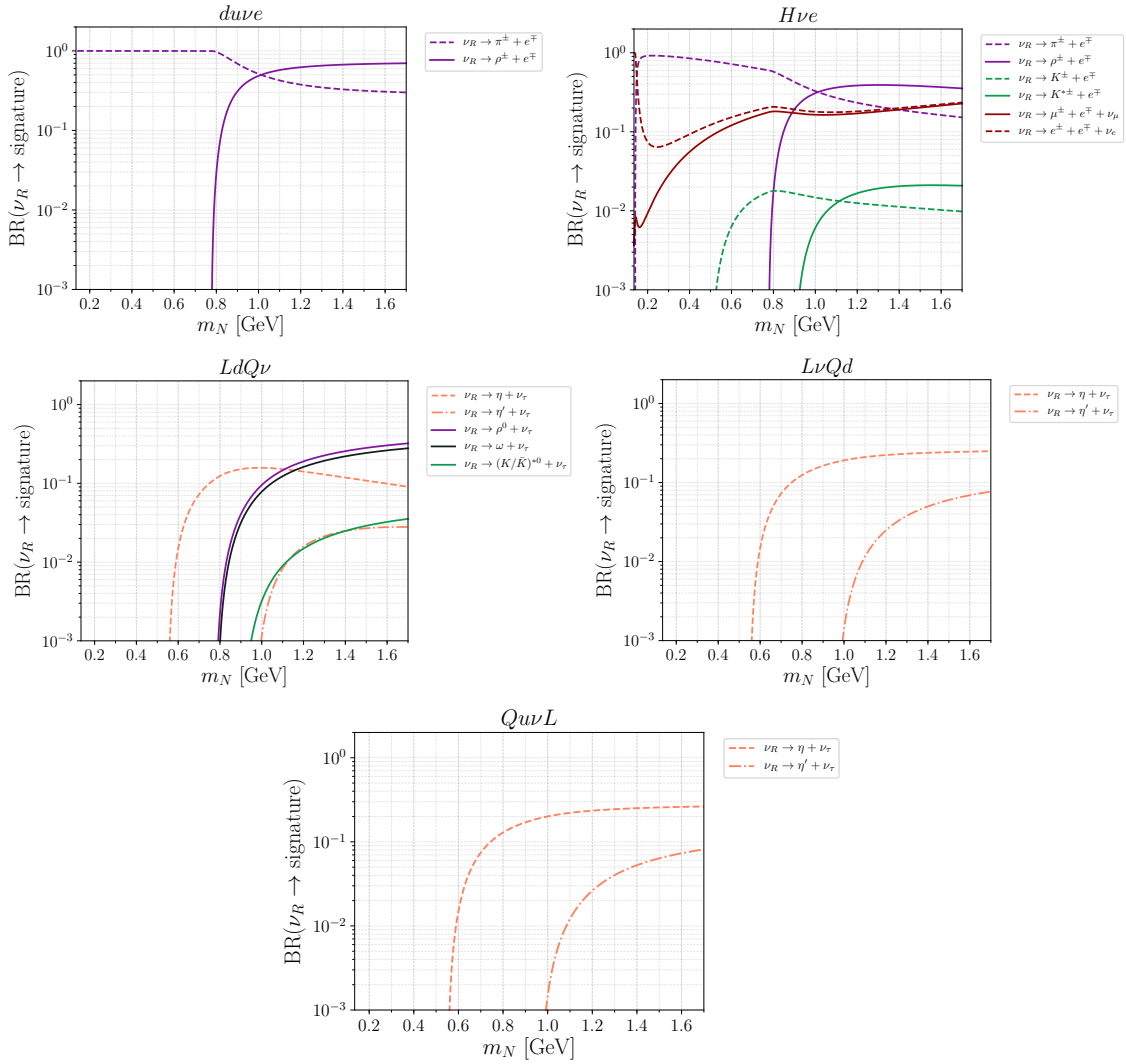


Figure 6. Branching ratios of visible decay modes for the sterile neutrino in ν SMEFT scenarios.

4 Experiment and Simulation

Belle II is an ongoing experiment at the SuperKEKB accelerator, which is an electron-positron collider operated at a relatively low center-of-mass energy $\sqrt{s} = 10.58$ GeV, *i.e.* at the $\Upsilon(4s)$ resonance. At Belle II an electron beam of energy 7 GeV collides asymmetrically with a positron beam of energy 4 GeV. With a projected 50 ab^{-1} integrated luminosity, besides the large number of B -mesons, Belle II is expected to produce inclusively 4.6×10^{10} tau pairs, via $e^-e^+ \rightarrow \tau^-\tau^+$. These events can be easily tagged, if one of the two τ 's decays into one prong. Given the clean environment and the large production rates of the τ 's, Belle II provides an ideal avenue for studying rare τ -decays.

For the purpose of this work, we study rare τ decays into a sterile neutrino, associated with either a charged meson or a charged lepton, plus missing energy from an escaping active neutrino. For the minimal scenario, the sterile neutrino is considered to be mixed

with the ν_τ only, while for the EFT scenarios with higher-dimensional operators the sterile neutrino is assumed to have four-fermion interactions with at least one third-generation lepton at the low-energy scale. We focus on the case that the sterile neutrinos are long-lived and decay to lighter mesons or leptons, disconnected from the production vertex, but within the tracker. We propose a displaced-vertex (DV) search strategy for these reactions, which requires at least two charged final-state particles for the signature. More concretely, the two displaced tracks can stem either directly from the decay of the long-lived sterile neutrino, or from the subsequent *prompt* decay of a meson, such as ρ^0 and η , produced from the sterile neutrino’s decay.

We now explain the event selections we impose for this search. We define a fiducial volume of the Belle II detector by $10\text{ cm} < r < 80\text{ cm}$ and $-40\text{ cm} < z < 120\text{ cm}$, where r and z are the transverse and longitudinal distances to the IP, respectively. The positive z direction is defined to be on the side of the incoming positron beam. The choice of $r > 10\text{ cm}$ ensures that the background events from K_S decays, prompt tracks, as well as detector material interactions are removed. The sterile neutrino is required to decay inside the fiducial volume. Second, in general we expect the tracking efficiency to deteriorate with increasing (transverse) distance from the IP inside the tracker. To parameterize this effect, we apply a naive linear function to interpolate the displaced-tracking efficiency, ranging from 100% at $r = 10\text{ cm}$ to 0% at $r = 80\text{ cm}$; see also Refs. [64, 73].

The efficiency to reconstruct a DV relies on the final-state tracks. For the case of two tracks stemming from a DV, we follow Ref. [69] to take this DV reconstruction efficiency to be 12%. With any π^0 , K^0 , or photon *additional* to the two tracks in the sterile neutrino decay products, the DV reconstruction efficiency is further multiplied with 70%. Similarly, for any additional pair of charged pions, the efficiency is modified by a factor of 85%^{4 5}.

On top of all these cuts and efficiencies, we expect that a more detailed analysis including all detector effects can remove the remaining SM background events, while retaining about 75% of the signal events. We therefore apply an overall efficiency of 75% on top of the previously mentioned factors. This estimate is inspired by Ref. [61], where the authors showed that by computation with the four-momenta of the final-state particles it is possible to derive the τ energy and the LLP mass up to a two-fold ambiguity at Belle II. By comparing their distributions it is possible to remove the entire background events while keeping $\gtrsim 75\%$ of all the signal events.

The final expected signal-event number can thus be computed as:

$$N_S = 2 \cdot N_{\tau\bar{\tau}} \cdot \text{BR}(\tau \rightarrow 1 \text{ prong}) \cdot \text{BR}(\tau \rightarrow \nu_R + X_1) \cdot \epsilon \cdot \text{BR}(\nu_R \rightarrow \text{visible}), \quad (4.1)$$

⁴These efficiencies are conservative estimates based on track finding efficiency investigations of the B-factory experiment BABAR (see Ref. [82, 83]). With the help of various Monte-Carlo event generators the efficiencies of reconstructing processes such as $e^+e^- \rightarrow \tau^+\tau^-$, $e^+e^- \rightarrow \pi^+\pi^-(\pi^+\pi^-\gamma)_{ISR}$, where γ_{ISR} is a high energetic photon emitted from an initial lepton, and hadronic decay modes are evaluated and compared to data of each BABAR run.

⁵To apply the analysis to reduce background events described in the following paragraph, the final state must be reconstructed as detailed as possible. Due to the unobservable neutrino in the final state we can not fully reconstruct it, but every other charged particle should be tracked.

where $N_{\tau\bar{\tau}} = 4.6 \times 10^{10}$, $\text{BR}(\tau \rightarrow 1 \text{ prong}) \approx 85\%$, and ϵ denotes the final event selection efficiency. The factor 2 arises because in each signal event two τ 's are produced, which can potentially each decay into a sterile neutrino. $\text{BR}(\nu_R \rightarrow \text{visible})$ is the decay branching ratio of the sterile neutrino into at least two charged particles. This excludes final states X_2 (see Table 2) consisting of neutrinos only, involving π^0 , which decays mostly into two photons, or involving K^0 (*i.e.* K_S or K_L), which is itself also long-lived and hence predominantly escapes the detector's fiducial volume.

We perform Monte-Carlo simulations with `Pythia8.245`, in order to numerically determine the event selection efficiencies ϵ for each benchmark scenario. `Pythia8` can generate $e^-e^+ \rightarrow \tau^-\tau^+$ events including the effects of ISR (initial state radiation) and FSR (final state radiation). The simulated τ 's are all exclusively set to decay to $\nu_R + X_1$, according to the computed branching ratios of $\text{BR}(\tau \rightarrow \nu_R + X_1)$ for different candidates of X_1 , *cf.* Table 2. With `Pythia8` providing the kinematics of each simulated sterile neutrino, we estimate its decay probability inside the fiducial volume folded with the linear displaced-tracking efficiency. The DV reconstruction efficiencies which depend on the final state particles are then multiplied with the cutflow efficiency, according to the various sterile neutrino decay branching ratios. At the end, we include the final overall efficiency 75% for removing the background events.

5 Numerical Results

As discussed in Sec. 4, with the proposed search strategy, and for 50 ab^{-1} integrated luminosity, we expect vanishing background at Belle II. In our numerical results, we show three-signal-event isocurves as the exclusion limits at 95% confidence level, and also as a measure of sensitivity of the experiment to the ν_R -models.

In Fig. 7, we present the sensitivity limits for the minimal scenario, *cf.* Sec. 3.1, shown in the plane $|U_{\tau 4}|^2$ vs. m_N . We find general agreement with the exclusion limits obtained in Ref. [61]. We also compare our limits with existing bounds obtained by the DELPHI [34] (marked dark gray) and CHARM [29, 30] (marked medium gray) experiments, respectively. Moreover, recently Ref. [84] has performed a re-analysis of the CHARM search results [29, 85], obtaining updated bounds on $|U_{\tau 4}|^2$ in the sterile neutrino mass range $290 \text{ MeV} < m_N < 1.6 \text{ GeV}$. We have included these exclusion limits in Fig. 7, shown in light gray. We find most of the parameter space that Belle II is sensitive to has now been excluded, except a relatively limited region at $1.2 \text{ GeV} \lesssim m_N \lesssim 1.7 \text{ GeV}$ for $|U_{\tau 4}|^2 \sim \mathcal{O}(10^{-4})$. For values of $|U_{\tau 4}|^2$ smaller than the Belle II limits, the production rates of the sterile neutrinos become too small and the sterile neutrinos are too long-lived to decay inside the detector fiducial volume, resulting in fewer than three signal events predicted. The left and right ends of the exclusion limits are determined by kinematical thresholds. At $m_N \sim 1.0 \text{ GeV}$ the isocurve displays a kink. This is due to the threshold of a τ -decay mode into a sterile neutrino and a rho-meson.

The Belle II exclusion limits for the various EFT operators listed in Sec. 2 are presented in Fig. 8, in the plane Λ vs. m_N . The left plot collects results for operators that are sensitive to neutrino masses below $\sim m_\eta$ as they induce sterile neutrino decays into pions

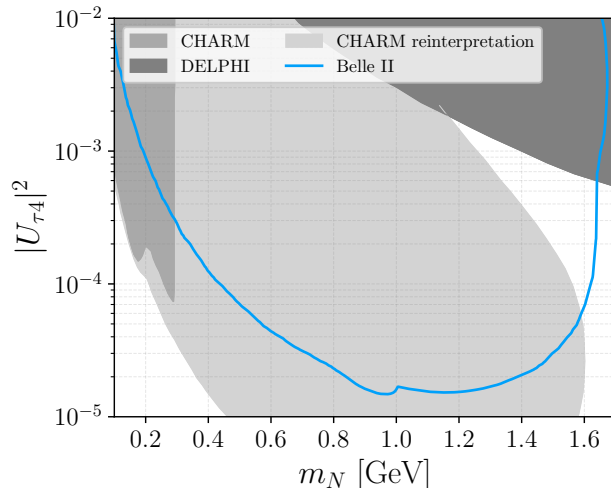


Figure 7. Expected sensitivity limits on the mixing matrix element squared, $|U_{\tau 4}|^2$, as function of the sterile neutrino mass, for the minimal scenario. The dark and medium gray areas correspond to the parameter regions currently excluded by DELPHI [34] and CHARM [29, 30], respectively. A recent re-interpretation [84] of the CHARM experiment results [29, 85] further excludes the light gray parameter region. The kink at $m_N \sim 1$ GeV is due to the ρ -threshold in the τ -decay.

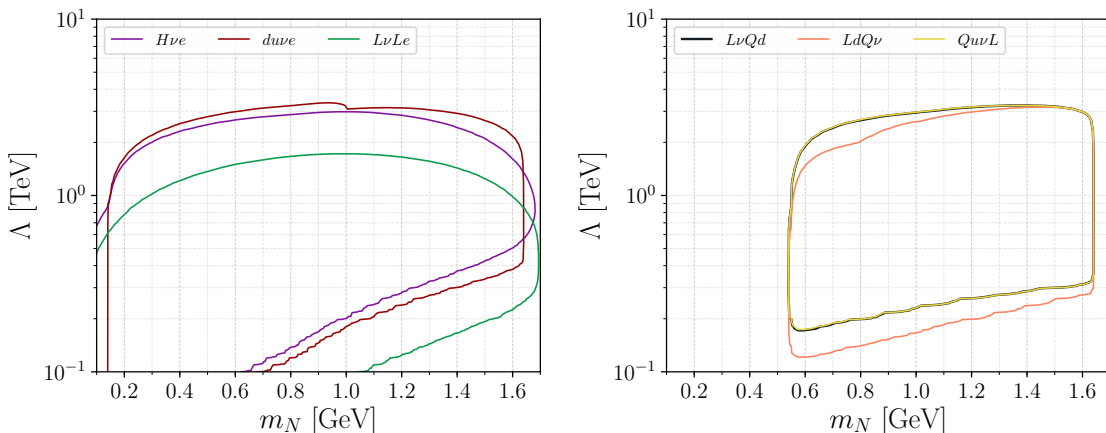


Figure 8. Sensitivity limits for the various EFT scenarios. We fix the Wilson coefficients at 1 and show projected bounds on the new-physics scale, Λ , as functions of m_N .

or charged leptons. The right plot displays operators that are insensitive to sterile neutrino masses below $\sim m_\eta$. We find the $C_{L\nu Qd}$ (black) and $C_{Q\nu wL}$ (yellow) sensitivities are almost identical, because the production and decay rates of the sterile neutrinos are similar (*cf.* Eqs. (2.6)-(2.9) and Eq. (A.2)). In general, we find all the six considered operators can be probed up to $\sim 1 - 3$ TeV in Λ across the sensitive mass ranges in the long-lived regime (large Λ). For even larger Λ values, the sterile neutrino lifetime would become so long that they decay only after traversing the detector and their production rates are also reduced too much, while for $\Lambda \lesssim 100$ GeV they decay before reaching the fiducial volume. For such small values of Λ the ν SMEFT framework is inapplicable. For the same reason as in the

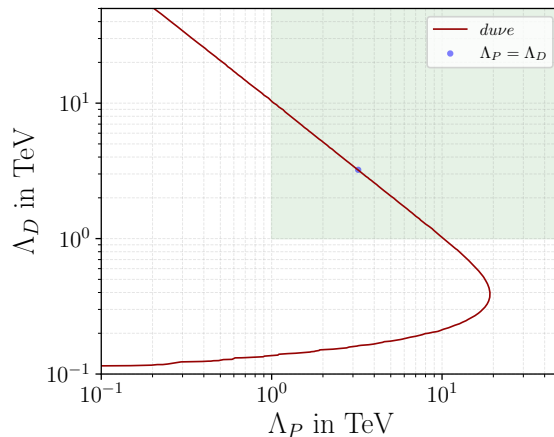


Figure 9. Sensitivity limits for the *duve* scenario for a fixed neutrino mass $m_N = 0.8$ GeV. The respective Wilson coefficients are fixed to 1, allowing to show projected bounds on the new physics scales Λ_P and Λ_D responsible for production and decay of the neutrino, respectively. Further included are a green area marking the parameter region $\Lambda_{P/D} \geq 1$ TeV, for which the ν SMEFT framework is applicable, and a blue dot depicting the limit for $\Lambda_P = \Lambda_D$ corresponding to the limit of Fig. 8 at 0.8 GeV.

minimal scenario (see Fig. 7) we observe a kink at m_N about 1.0 GeV in the long-lived regime for the \mathcal{O}_{duve} and $\mathcal{O}_{LdQ\nu}$ operators. For $LdQ\nu$ the kink is not as pronounced as in *duve* or the minimal scenario. Comparing the $\tau \rightarrow \nu_R + (\pi, \rho)$ branching ratios (see Fig. 4) for the EFT operators, we see that the rho branching ratio of *duve* quickly dominates the $m_N \lesssim 1$ GeV region over the pion branching ratio, whereas for $LdQ\nu$ the rho only overtakes for $m_N \lesssim 0.6$ GeV. Thus, the kink is less pronounced in this scenario.

In general UV-complete scenarios, several EFT operators can be induced simultaneously. In such scenarios the limits could change somewhat from our results here. While a general scan is not very useful, we have estimated what happens in a specific scenario where we have independent couplings for the production and decay of the sterile neutrino. In Fig. 8 we show constraints as a function of m_N for the choice $C_{duve}^{11\nu_R^3} = C_{duve}^{11\nu_R^1}$, where the first (second) coupling dominates the production (decay) of the sterile neutrino. We label the corresponding Λ 's by Λ_P (for production) and Λ_D (for decay). For a fixed sterile neutrino mass of $m_N = 0.8$ GeV, we investigated what happened if we freely vary the two couplings. We observe that in the window where $\Lambda_{P,D} \geq 1$ TeV (where the EFT is valid) the constraints on the individual couplings can be strengthened by roughly a factor of 3, at the cost of a reduced sensitivity to the other coupling. With the expected sensitivities we therefore do not expect a significant difference in sensitivity for scenarios with more EFT couplings. Of course, specific UV-complete models can be studied in detail by matching to our EFT operators.

To the best of our knowledge, no other constraints on these EFT couplings have been established for sterile neutrino masses in this region. For sterile neutrino masses below 100 MeV, several operators considered in this work have been constrained from LHC searches for tau production plus missing transverse energy [86]. The resulting constraints are at the

TeV level as well, but, as mentioned above, require lighter sterile neutrinos in order for them to traverse the LHC detectors. In addition, constraints from meson decays, tau decays, lepton flavor universality, CKM unitarity, β -decays, and $EC\nu NS$, have been discussed in Refs. [86–93], where either a massless sterile neutrino was assumed, or ν SMEFT operators with flavor configurations different from those we have studied here were considered. Consequently, these constraints are not shown in Fig. 8.

6 Conclusions

At Belle II, $10^{10} - 10^{11}$ tau leptons are predicted to be produced with an integrated luminosity of 50 ab^{-1} over the whole experiment lifetime, making it possible to search for rare τ decays. In this work, we have proposed a strategy based on displaced vertex at Belle II, to search for long-lived sterile neutrinos produced from τ decays. The search includes a requirement on the fiducial volume consisting of the tracker and a linear displaced-tracking efficiency. Further, to reconstruct the displaced vertices, we apply realistic efficiency factors depending on the final states of the sterile neutrino decays. Finally, based on existing literature [61, 69], an overall factor of 75% is imposed to account for removing the remaining background events.

We have not only considered the minimal scenario where the sterile neutrinos are produced and decaying via the same mixing parameter, $|U_{\tau 4}|^2$, but also worked in the framework of the Standard Model Effective Field Theory extended with sterile neutrinos encoding the effects of heavy new physics into non-renormalizable operators with dimensions up to six. Following the proposed search strategy, we obtained the sensitivity limits of Belle II to these theoretical scenarios. In the minimal scenario, our results are in general agreement with those obtained in Ref. [61]. For the EFT scenarios, we switch on one EFT operator at a time, and assume the type-I seesaw relation allowing us to disregard the weak interactions with the mixing parameter which is too small to affect the phenomenology. We find that with our search strategy for the various ν SMEFT operators considered, Belle II can probe the new-physics scale up to about 3 TeV, assuming unity Wilson coefficients, in the kinematically allowed mass range, proving Belle II has unique sensitivities to ν SMEFT interactions with third-generation leptons.

Acknowledgements

We thank Florian Bernlochner, Claudio Dib, Juan Carlos Helo, Nicolás Neill, Maksym Ovchinnikov, Abner Soffer, and Arsenii Titov for useful discussions. Z.S.W. is supported by the Ministry of Science and Technology (MoST) of Taiwan with grant numbers MoST-109-2811-M-007-509 and MoST-110-2811-M-007-542-MY3. Financial support for H.K.D. by the DFG (CRC 110, “Symmetries and the Emergence of Structure in QCD”) is gratefully acknowledged.

meson M_P	f_M [MeV]	meson M_V	f_M^V [MeV]
K^\pm	155.6 [94]	$K^{*\pm}$	230 [95]
π^\pm	130.2 [94]	ρ^\pm	209 [96]

Table 3. Decay constants for charged pseudoscalar and vector mesons.

A Two-body Decay Processes with a Sterile Neutrino

A.1 Charged Currents

Via the charged-current interactions introduced in Eq. (2.5), the τ lepton and sterile neutrino can undergo two-body decays into final states consisting of a lepton and a charged pseudoscalar or vector meson. For a pseudoscalar meson M_{ij} consisting of the valence quarks, \bar{q}_i and q_j , we define the matrix element for the axial-vector current as

$$\langle 0 | \bar{q}_i \gamma^\mu \gamma^5 q_j | M_{ij}(q) \rangle \equiv i q^\mu f_{M_{ij}}, \quad (\text{A.1})$$

where q is the momentum of M_{ij} and $f_{M_{ij}}$ is the decay constant. After applying the equation of motion to the current, we define the decay constant for the axial current,

$$\langle 0 | \bar{q}_i \gamma^5 q_j | M_{ij}(q) \rangle = i \frac{m_{M_{ij}}^2}{m_{q_i} + m_{q_j}} f_{M_{ij}} \equiv i f_{M_{ij}}^S, \quad (\text{A.2})$$

where m_{q_i} and $m_{M_{ij}}$ are the masses of quark q_i and pseudoscalar meson M_{ij} , respectively. The matrix elements of the vector and tensor currents with a vector meson are given as:

$$\begin{aligned} \langle 0 | \bar{q}_i \gamma^\mu q_j | M_{ij}^*(q, \epsilon) \rangle &\equiv i f_{M_{ij}}^V m_{M_{ij}^*} \epsilon^\mu, \\ \langle 0 | \bar{q}_i \sigma^{\mu\nu} q_j | M_{ij}^*(q, \epsilon) \rangle &\equiv -f_{M_{ij}}^T (q^\mu \epsilon^\nu - q^\nu \epsilon^\mu), \end{aligned} \quad (\text{A.3})$$

where $M_{ij}^*(q, \epsilon)$ denotes a vector meson with mass $m_{M_{ij}^*}$, momentum q , and polarization vector ϵ , and we assume $f_{M_{ij}}^T \simeq f_{M_{ij}}^V$. We list the values of all the relevant decay constants in Table 3.

A.2 Neutral Currents

A.2.1 The Two-body Decay of the Sterile Neutrino in the Minimal Model

In the minimal model, the sterile neutrino can decay into a neutral pseudoscalar meson M_P^0 or vector meson M_V^0 via the mixing with ν_τ . The decay width of $\nu_R \rightarrow \nu_\tau + M_P^0$ can be written as [51]

$$\Gamma(\nu_R \rightarrow \nu_\tau M_{a,P}^0) = 2 \times \frac{G_F^2 f_a^2 m_N^3 |U_{\tau 4}|^2}{32\pi} \left(1 - \frac{m_a^2}{m_N^2}\right)^2, \quad (\text{A.4})$$

where a denotes π^0, η , or η' , m_a is the mass of meson $M_{a,P}^0$, and we include a factor 2 explicitly to account for the charge-conjugated decay modes of the Majorana sterile neutrino (similarly for the other decay rates expressions given below). For $\nu_R \rightarrow \nu_\tau + M_V^0$, the decay rates are [51]

$$\Gamma(\nu_R \rightarrow \nu_\tau M_{a,V}^0) = 2 \times \frac{G_F^2 f_a^2 g_a^2 |U_{\tau 4}|^2 m_N^3}{32\pi} \left(1 + 2 \frac{m_a^2}{m_N^2}\right) \left(1 - \frac{m_a^2}{m_N^2}\right)^2, \quad (\text{A.5})$$

meson M^0	f_a [MeV]	g_a
ρ^0	220.6 [97]	$1 - 2 \sin^2 \theta_w$
ω	198 [97]	$-\frac{2}{3} \sin^2 \theta_w$
ϕ	227.4 [97]	$\sqrt{2}(-\frac{1}{2} + \frac{2}{3} \sin^2 \theta_w)$
η	81.7 [98]	Not applicable
η'	-94.7 [98]	
π^0	130 [97]	

Table 4. Decay constants and g_a of neutral mesons.

where $a = \rho^0, \omega$, or ϕ , and m_a labels the mass of meson $M_{a,V}^0$. In Table 4, we list the values of f_a and g_a we use for the numerical studies in this work.

A.2.2 The Two-body Decay of the Sterile Neutrino via higher-dimensional Operators

Some neutral-current interactions listed in Eq. (2.6) include a sterile neutrino and two quarks, and can hence induce decays of the sterile neutrino into a neutral pseudoscalar meson. We reproduce them here:

$$\mathcal{L}_{NC} = \frac{2G_F}{\sqrt{2}} (\bar{u}_R u_L \bar{\nu}_L C_{SLR}^{NC} \nu_R + \bar{d}_L d_R \bar{\nu}_L C_{SRR}^{NC1} \nu_R) + \text{h.c.} \quad (\text{A.6})$$

To compute the decay rates of the sterile neutrino via these terms, we work in the $SU(3)$ chiral perturbation theory, following the calculation procedure as detailed in Ref. [99]. We first write down the leading-order chiral Lagrangian containing the Lorentz- and chiral-invariant terms with the lowest number of derivatives,

$$\mathcal{L}_{\pi,K} = \frac{F^2}{4} \text{Tr} [(D_\mu U)^\dagger (D^\mu U)] + \frac{F^2}{4} \text{Tr} [U^\dagger \chi + U \chi^\dagger], \quad (\text{A.7})$$

where $D_\mu U = \partial_\mu U - i l_\mu U + i U r_\mu$ and $\chi = 2B(M + s - ip)$. l_μ, r_μ, s, p are external sources and $M = \text{diag}(m_u, m_d, m_s)$ is a diagonal 3×3 quark mass matrix. U is given by

$$U(x) = \exp\left(\frac{i\sqrt{2}\Pi(x)}{F}\right), \quad \Pi(x) = \begin{pmatrix} \frac{\pi^0}{\sqrt{2}} + \frac{\eta_8}{\sqrt{6}} + \frac{\eta_0}{\sqrt{3}} & \pi^+ & K^+ \\ \pi^- & -\frac{\pi^0}{\sqrt{2}} + \frac{\eta_8}{\sqrt{6}} + \frac{\eta_0}{\sqrt{3}} & K^0 \\ K^- & \bar{K}^0 & -\sqrt{\frac{2}{3}}\eta_8 + \frac{\eta_0}{\sqrt{3}} \end{pmatrix}. \quad (\text{A.8})$$

η_8 and η_0 are in the singlet-octet basis and their relations with the physical states η and η' are

$$\begin{pmatrix} \eta \\ \eta' \end{pmatrix} = \frac{1}{F} \begin{pmatrix} F_8 \cos \theta_8 & -F_0 \sin \theta_8 \\ F_8 \sin \theta_8 & F_0 \cos \theta_8 \end{pmatrix} \begin{pmatrix} \eta_8 \\ \eta_0 \end{pmatrix}. \quad (\text{A.9})$$

The values of the relevant parameters are [99, 100]

$$\begin{aligned} F &= 92.2 \text{ MeV}, & F_0 &= 118.1 \text{ MeV}, & F_8 &= 133.8 \text{ MeV}, \\ \theta_8 &= -11.0^\circ, & \theta_0 &= -26.7^\circ. \end{aligned} \quad (\text{A.10})$$

By using the external source field method, we find

$$\begin{aligned} s + ip &= \frac{-2G_F}{\sqrt{2}} \left\{ \bar{\nu}_\tau c_{\text{SLR}}^{NC} \nu_R + (\bar{\nu}_\tau c_{\text{SRR}}^{NC1} \nu_R)^\dagger \right\}, \\ s - ip &= (s + ip)^\dagger. \end{aligned} \quad (\text{A.11})$$

To obtain the decay rates of the sterile neutrino, we insert these currents into Eq. (A.7) and expand U to leading order.

The neutral tensor current in Eq. (2.6) leads to the decay of the sterile neutrino into a vector meson. We define the following matrix element:

$$\langle 0 | \bar{q}_1 \sigma^{\mu\nu} d | M_V^0(q, \epsilon) \rangle \equiv -f_M^T (q^\mu \epsilon^\nu - q^\nu \epsilon^\mu), \quad (\text{A.12})$$

where q_1 can be a down or strange quark, d is a down quark, and $M_V^0 = \rho^0, \omega, K^{*0}$. The tensor decay constants f_M^T are related to the vector decay constants by $f_{\rho^0}^T = f_{\rho^\pm} / \sqrt{2}$, $f_\omega^T = f_\omega / \sqrt{2}$, and $f_{K^{*0}}^T = f_{K^{*\pm}}$.

B Three-body Decays

In the minimal scenario, the sterile neutrino can decay into three light active neutrinos, and the corresponding decay rates can be expressed in a closed form [80]

$$\Gamma(\nu_R \rightarrow \nu_\tau \nu_\beta \bar{\nu}_\beta) = 2 \times (1 + \delta_{\tau\beta}) \frac{G_F^2 m_N^5 |U_{\tau 4}|^2}{768 \pi^3}, \quad (\text{B.1})$$

where $\beta = e, \mu, \tau$ is the flavor of light neutrinos. However, in most cases the three-body decay widths cannot be computed analytically. Thus, we compute these three-body phase space integrals numerically. With the help of `FeynCalc` [101–103] and the method explained in Appendix B of Ref. [51], we automatize the calculation procedure in `Mathematica`.

References

- [1] P. F. de Salas, D. V. Forero, S. Gariazzo, P. Martínez-Miravé, O. Mena, C. A. Ternes, M. Tórtola, and J. W. F. Valle, *2020 global reassessment of the neutrino oscillation picture*, *JHEP* **02** (2021) 071, [[arXiv:2006.11237](#)].
- [2] P. Minkowski, $\mu \rightarrow e\gamma$ at a Rate of One Out of 10^9 Muon Decays?, *Phys. Lett. B* **67** (1977) 421–428.
- [3] T. Yanagida, *Horizontal gauge symmetry and masses of neutrinos*, *Conf. Proc. C* **7902131** (1979) 95–99.
- [4] R. N. Mohapatra and G. Senjanovic, *Neutrino Mass and Spontaneous Parity Nonconservation*, *Phys. Rev. Lett.* **44** (1980) 912.
- [5] M. Gell-Mann, P. Ramond, and R. Slansky, *Complex Spinors and Unified Theories*, *Conf. Proc. C* **790927** (1979) 315–321, [[arXiv:1306.4669](#)].
- [6] J. Schechter and J. Valle, *Neutrino Masses in $SU(2) \times U(1)$ Theories*, *Phys. Rev. D* **22** (1980) 2227.

- [7] W. Dekens, J. de Vries, K. Fuyuto, E. Mereghetti, and G. Zhou, *Sterile neutrinos and neutrinoless double beta decay in effective field theory*, *JHEP* **06** (2020) 097, [[arXiv:2002.07182](#)].
- [8] I. Esteban, M. C. Gonzalez-Garcia, M. Maltoni, T. Schwetz, and A. Zhou, *The fate of hints: updated global analysis of three-flavor neutrino oscillations*, *JHEP* **09** (2020) 178, [[arXiv:2007.14792](#)].
- [9] F. Capozzi, E. Di Valentino, E. Lisi, A. Marrone, A. Melchiorri, and A. Palazzo, *Global constraints on absolute neutrino masses and their ordering*, *Phys. Rev. D* **95** (2017), no. 9 096014, [[arXiv:2003.08511](#)]. [Addendum: *Phys.Rev.D* 101, 116013 (2020)].
- [10] M. Bando and K. Yoshioka, *Sterile neutrinos in a grand unified model*, *Prog. Theor. Phys.* **100** (1998) 1239–1250, [[hep-ph/9806400](#)].
- [11] F. Deppisch, S. Kulkarni, and W. Liu, *Heavy neutrino production via Z' at the lifetime frontier*, *Phys. Rev. D* **100** (2019), no. 3 035005, [[arXiv:1905.11889](#)].
- [12] C.-W. Chiang, G. Cottin, A. Das, and S. Mandal, *Displaced heavy neutrinos from Z' decays at the LHC*, *JHEP* **12** (2019) 070, [[arXiv:1908.09838](#)].
- [13] R. Mohapatra and J. C. Pati, *A Natural Left-Right Symmetry*, *Phys. Rev. D* **11** (1975) 2558.
- [14] J. C. Pati and A. Salam, *Lepton Number as the Fourth Color*, *Phys. Rev. D* **10** (1974) 275–289. [Erratum: *Phys.Rev.D* 11, 703–703 (1975)].
- [15] R. N. Mohapatra and G. Senjanovic, *Neutrino Masses and Mixings in Gauge Models with Spontaneous Parity Violation*, *Phys. Rev. D* **23** (1981) 165.
- [16] W.-Y. Keung and G. Senjanovic, *Majorana Neutrinos and the Production of the Right-handed Charged Gauge Boson*, *Phys. Rev. Lett.* **50** (1983) 1427.
- [17] I. Doršner, S. Fajfer, A. Greljo, J. F. Kamenik, and N. Košnik, *Physics of leptoquarks in precision experiments and at particle colliders*, *Phys. Rept.* **641** (2016) 1–68, [[arXiv:1603.04993](#)].
- [18] F. del Aguila, S. Bar-Shalom, A. Soni, and J. Wudka, *Heavy Majorana Neutrinos in the Effective Lagrangian Description: Application to Hadron Colliders*, *Phys. Lett. B* **670** (2009) 399–402, [[arXiv:0806.0876](#)].
- [19] A. Aparici, K. Kim, A. Santamaria, and J. Wudka, *Right-handed neutrino magnetic moments*, *Phys. Rev. D* **80** (2009) 013010, [[arXiv:0904.3244](#)].
- [20] Y. Liao and X.-D. Ma, *Operators up to Dimension Seven in Standard Model Effective Field Theory Extended with Sterile Neutrinos*, *Phys. Rev. D* **96** (2017), no. 1 015012, [[arXiv:1612.04527](#)].
- [21] N. F. Bell, V. Cirigliano, M. J. Ramsey-Musolf, P. Vogel, and M. B. Wise, *How magnetic is the Dirac neutrino?*, *Phys. Rev. Lett.* **95** (2005) 151802, [[hep-ph/0504134](#)].
- [22] M. L. Graesser, *Broadening the Higgs boson with right-handed neutrinos and a higher dimension operator at the electroweak scale*, *Phys. Rev.* **D76** (2007) 075006, [[arXiv:0704.0438](#)].
- [23] M. L. Graesser, *Experimental Constraints on Higgs Boson Decays to TeV-scale Right-Handed Neutrinos*, [arXiv:0705.2190](#).
- [24] **Belle** Collaboration, D. Liventsev et al., *Search for heavy neutrinos at Belle*, *Phys. Rev. D* **87** (2013), no. 7 071102, [[arXiv:1301.1105](#)]. [Erratum: *Phys.Rev.D* 95, 099903 (2017)].

- [25] G. Bernardi et al., *FURTHER LIMITS ON HEAVY NEUTRINO COUPLINGS*, *Phys. Lett. B* **203** (1988) 332–334.
- [26] O. Ruchayskiy and A. Ivashko, *Experimental bounds on sterile neutrino mixing angles*, *JHEP* **06** (2012) 100, [[arXiv:1112.3319](#)].
- [27] **L3** Collaboration, P. Achard et al., *Search for heavy isosinglet neutrino in e^+e^- annihilation at LEP*, *Phys. Lett. B* **517** (2001) 67–74, [[hep-ex/0107014](#)].
- [28] **T2K** Collaboration, K. Abe et al., *Search for heavy neutrinos with the T2K near detector ND280*, *Phys. Rev. D* **100** (2019), no. 5 052006, [[arXiv:1902.07598](#)].
- [29] **CHARM** Collaboration, F. Bergsma et al., *A Search for Decays of Heavy Neutrinos in the Mass Range 0.5-GeV to 2.8-GeV*, *Phys. Lett. B* **166** (1986) 473–478.
- [30] J. Orloff, A. N. Rozanov, and C. Santoni, *Limits on the mixing of tau neutrino to heavy neutrinos*, *Phys. Lett. B* **550** (2002) 8–15, [[hep-ph/0208075](#)].
- [31] **NuTeV**, **E815** Collaboration, A. Vaitaitis et al., *Search for neutral heavy leptons in a high-energy neutrino beam*, *Phys. Rev. Lett.* **83** (1999) 4943–4946, [[hep-ex/9908011](#)].
- [32] **NA3** Collaboration, J. Badier et al., *Mass and Lifetime Limits on New Longlived Particles in 300-GeV/ π^- Interactions*, *Z. Phys. C* **31** (1986) 21.
- [33] **WA66** Collaboration, A. M. Cooper-Sarkar et al., *Search for Heavy Neutrino Decays in the BEBC Beam Dump Experiment*, *Phys. Lett. B* **160** (1985) 207–211.
- [34] **DELPHI** Collaboration, P. Abreu et al., *Search for neutral heavy leptons produced in Z decays*, *Z. Phys. C* **74** (1997) 57–71. [Erratum: *Z.Phys.C* 75, 580 (1997)].
- [35] **LHCb** Collaboration, R. Aaij et al., *Search for massive long-lived particles decaying semileptonically in the LHCb detector*, *Eur. Phys. J. C* **77** (2017), no. 4 224, [[arXiv:1612.00945](#)].
- [36] S. Antusch, E. Cazzato, and O. Fischer, *Sterile neutrino searches via displaced vertices at LHCb*, *Phys. Lett. B* **774** (2017) 114–118, [[arXiv:1706.05990](#)].
- [37] **CMS** Collaboration, V. Khachatryan et al., *Search for heavy Majorana neutrinos in $\mu^\pm\mu^\pm + jets$ events in proton-proton collisions at $\sqrt{s} = 8$ TeV*, *Phys. Lett. B* **748** (2015) 144–166, [[arXiv:1501.05566](#)].
- [38] **CMS** Collaboration, A. M. Sirunyan et al., *Search for heavy neutral leptons in events with three charged leptons in proton-proton collisions at $\sqrt{s} = 13$ TeV*, *Phys. Rev. Lett.* **120** (2018), no. 22 221801, [[arXiv:1802.02965](#)].
- [39] **ATLAS** Collaboration, G. Aad et al., *Search for heavy Majorana neutrinos with the ATLAS detector in pp collisions at $\sqrt{s} = 8$ TeV*, *JHEP* **07** (2015) 162, [[arXiv:1506.06020](#)].
- [40] **ATLAS** Collaboration, G. Aad et al., *Search for heavy neutral leptons in decays of W bosons produced in 13 TeV pp collisions using prompt and displaced signatures with the ATLAS detector*, *JHEP* **10** (2019) 265, [[arXiv:1905.09787](#)].
- [41] **FASER** Collaboration, A. Ariga et al., *FASER’s physics reach for long-lived particles*, *Phys. Rev. D* **99** (2019), no. 9 095011, [[arXiv:1811.12522](#)].
- [42] D. Curtin et al., *Long-Lived Particles at the Energy Frontier: The MATHUSLA Physics Case*, *Rept. Prog. Phys.* **82** (2019), no. 11 116201, [[arXiv:1806.07396](#)].
- [43] L. Lee, C. Ohm, A. Soffer, and T.-T. Yu, *Collider Searches for Long-Lived Particles Beyond the Standard Model*, *Prog. Part. Nucl. Phys.* **106** (2019) 210–255, [[arXiv:1810.12602](#)].

- [44] J. Alimena et al., *Searching for long-lived particles beyond the Standard Model at the Large Hadron Collider*, *J. Phys. G* **47** (2020), no. 9 090501, [[arXiv:1903.04497](#)].
- [45] J. Beacham et al., *Physics Beyond Colliders at CERN: Beyond the Standard Model Working Group Report*, *J. Phys. G* **47** (2020), no. 1 010501, [[arXiv:1901.09966](#)].
- [46] F. Kling and S. Trojanowski, *Heavy Neutral Leptons at FASER*, *Phys. Rev. D* **97** (2018), no. 9 095016, [[arXiv:1801.08947](#)].
- [47] M. Hirsch and Z. S. Wang, *Heavy neutral leptons at ANUBIS*, *Phys. Rev. D* **101** (2020), no. 5 055034, [[arXiv:2001.04750](#)].
- [48] G. Cottin, J. C. Helo, M. Hirsch, A. Titov, and Z. S. Wang, *Heavy neutral leptons in effective field theory and the high-luminosity LHC*, [arXiv:2105.13851](#).
- [49] J. C. Helo, M. Hirsch, and Z. S. Wang, *Heavy neutral fermions at the high-luminosity LHC*, *JHEP* **07** (2018) 056, [[arXiv:1803.02212](#)].
- [50] D. Dercks, H. K. Dreiner, M. Hirsch, and Z. S. Wang, *Long-Lived Fermions at AL3X*, *Phys. Rev. D* **99** (2019), no. 5 055020, [[arXiv:1811.01995](#)].
- [51] J. De Vries, H. K. Dreiner, J. Y. Günther, Z. S. Wang, and G. Zhou, *Long-lived Sterile Neutrinos at the LHC in Effective Field Theory*, *JHEP* **03** (2021) 148, [[arXiv:2010.07305](#)].
- [52] A. Das, S. Jana, S. Mandal, and S. Nandi, *Probing right handed neutrinos at the LHeC and lepton colliders using fat jet signatures*, *Phys. Rev. D* **99** (2019), no. 5 055030, [[arXiv:1811.04291](#)].
- [53] G. Cottin, O. Fischer, S. Mandal, M. Mitra, and R. Padhan, *Displaced Neutrino Jets at the LHeC*, [arXiv:2104.13578](#).
- [54] S. Antusch, O. Fischer, and A. Hammad, *Lepton-Trijet and Displaced Vertex Searches for Heavy Neutrinos at Future Electron-Proton Colliders*, *JHEP* **03** (2020) 110, [[arXiv:1908.02852](#)].
- [55] O. Fischer and S. Antusch, *Searches for Sterile Neutrinos at Future Electron-Proton Colliders*, *PoS DIS2017* (2018) 090, [[arXiv:1709.00880](#)].
- [56] S. Antusch, E. Cazzato, and O. Fischer, *Sterile neutrino searches at future e^-e^+ , pp , and e^-p colliders*, *Int. J. Mod. Phys. A* **32** (2017), no. 14 1750078, [[arXiv:1612.02728](#)].
- [57] S. Antusch, E. Cazzato, and O. Fischer, *Displaced vertex searches for sterile neutrinos at future lepton colliders*, *JHEP* **12** (2016) 007, [[arXiv:1604.02420](#)].
- [58] S. Antusch and O. Fischer, *Testing sterile neutrino extensions of the Standard Model at future lepton colliders*, *JHEP* **05** (2015) 053, [[arXiv:1502.05915](#)].
- [59] **Belle-II** Collaboration, W. Altmannshofer et al., *The Belle II Physics Book*, *PTEP* **2019** (2019), no. 12 123C01, [[arXiv:1808.10567](#)]. [Erratum: *PTEP* 2020, 029201 (2020)].
- [60] A. Kobach and S. Dobbs, *Heavy Neutrinos and the Kinematics of Tau Decays*, *Phys. Rev. D* **91** (2015), no. 5 053006, [[arXiv:1412.4785](#)].
- [61] C. O. Dib, J. C. Helo, M. Nayak, N. A. Neill, A. Soffer, and J. Zamora-Saa, *Searching for a sterile neutrino that mixes predominantly with ν_τ at B factories*, *Phys. Rev. D* **101** (2020), no. 9 093003, [[arXiv:1908.09719](#)].
- [62] J. Heck and W. Rodejohann, *Lepton flavor violation with displaced vertices*, *Phys. Lett. B* **776** (2018) 385–390, [[arXiv:1710.02062](#)].

- [63] F. Tenchini, M. Garcia-Hernandez, T. Kraetzschmar, P. K. Rados, E. De La Cruz-Burelo, A. De Yta-Hernandez, I. Heredia de la Cruz, and A. Rostomyan, *First results and prospects for tau LFV decay $\tau \rightarrow e + \alpha(\text{invisible})$ at Belle II*, *PoS ICHEP2020* (2021) 288.
- [64] K. Cheung, A. Soffer, Z. S. Wang, and Y.-H. Wu, *Probing charged lepton flavor violation with axion-like particles at Belle II*, [arXiv:2108.11094](#).
- [65] J. T. Daub, H. K. Dreiner, C. Hanhart, B. Kubis, and U. G. Meissner, *Improving the Hadron Physics of Non-Standard-Model Decays: Example Bounds on R-parity Violation*, *JHEP* **01** (2013) 179, [[arXiv:1212.4408](#)].
- [66] H. K. Dreiner, K. Nickel, F. Staub, and A. Vicente, *New bounds on trilinear R-parity violation from lepton flavor violating observables*, *Phys. Rev. D* **86** (2012) 015003, [[arXiv:1204.5925](#)].
- [67] C. S. Kim, Y. Kwon, D. Lee, S. Oh, and D. Sahoo, *Probing sterile neutrinos in B(D) meson decays at Belle II (BESIII)*, *Eur. Phys. J. C* **80** (2020), no. 8 730, [[arXiv:1908.00376](#)].
- [68] M. Duerr, T. Ferber, C. Hearty, F. Kahlhoefer, K. Schmidt-Hoberg, and P. Tunney, *Invisible and displaced dark matter signatures at Belle II*, *JHEP* **02** (2020) 039, [[arXiv:1911.03176](#)].
- [69] S. Dey, C. O. Dib, J. Carlos Helo, M. Nayak, N. A. Neill, A. Soffer, and Z. S. Wang, *Long-lived light neutralinos at Belle II*, *JHEP* **02** (2021) 211, [[arXiv:2012.00438](#)].
- [70] M. Duerr, T. Ferber, C. Garcia-Cely, C. Hearty, and K. Schmidt-Hoberg, *Long-lived Dark Higgs and Inelastic Dark Matter at Belle II*, *JHEP* **04** (2021) 146, [[arXiv:2012.08595](#)].
- [71] A. Filimonova, R. Schäfer, and S. Westhoff, *Probing dark sectors with long-lived particles at BELLE II*, *Phys. Rev. D* **101** (2020), no. 9 095006, [[arXiv:1911.03490](#)].
- [72] X. Chen, Z. Hu, Y. Wu, and K. Yi, *Search for dark photon and dark matter signatures around electron-positron colliders*, *Phys. Lett. B* **814** (2021) 136076, [[arXiv:2001.04382](#)].
- [73] E. Bertholet, S. Chakraborty, V. Loldzde, T. Okui, A. Soffer, and K. Tobioka, *Heavy QCD Axion at Belle II: Displaced and Prompt Signals*, [arXiv:2108.10331](#).
- [74] D. W. Kang, P. Ko, and C.-T. Lu, *Exploring properties of long-lived particles in inelastic dark matter models at Belle II*, *JHEP* **04** (2021) 269, [[arXiv:2101.02503](#)].
- [75] M. Acevedo, A. Blackburn, N. Blinov, B. Shuve, and M. Stone, *Multi-track Displaced Vertices at B-Factories*, [arXiv:2105.12744](#).
- [76] S. Dreyer et al., *Physics reach of a long-lived particle detector at Belle II*, [arXiv:2105.12962](#).
- [77] B. Grzadkowski, M. Iskrzynski, M. Misiak, and J. Rosiek, *Dimension-Six Terms in the Standard Model Lagrangian*, *JHEP* **10** (2010) 085, [[arXiv:1008.4884](#)].
- [78] J. M. Butterworth, M. Chala, C. Englert, M. Spannowsky, and A. Titov, *Higgs phenomenology as a probe of sterile neutrinos*, *Phys. Rev. D* **100** (2019), no. 11 115019, [[arXiv:1909.04665](#)].
- [79] B. Canas, O. Miranda, A. Parada, M. Tortola, and J. W. Valle, *Updating neutrino magnetic moment constraints*, *Phys. Lett. B* **753** (2016) 191–198, [[arXiv:1510.01684](#)]. [Addendum: *Phys.Lett.B* 757, 568–568 (2016)].
- [80] K. Bondarenko, A. Boyarsky, D. Gorbunov, and O. Ruchayskiy, *Phenomenology of GeV-scale Heavy Neutral Leptons*, *JHEP* **11** (2018) 032, [[arXiv:1805.08567](#)].

- [81] R. Beltrán, G. Cottin, J. C. Helo, M. Hirsch, A. Titov, and Z. S. Wang, *Long-lived heavy neutral leptons at the LHC: four-fermion single- N_R operators*, [arXiv:2110.15096](#).
- [82] T. Allmendinger et al., *Track Finding Efficiency in BaBar*, *Nucl. Instrum. Meth. A* **704** (2013) 44–59, [[arXiv:1207.2849](#)].
- [83] **BaBar** Collaboration, B. Aubert et al., *The BABAR Detector: Upgrades, Operation and Performance*, *Nucl. Instrum. Meth. A* **729** (2013) 615–701, [[arXiv:1305.3560](#)].
- [84] I. Boiarska, A. Boyarsky, O. Mikulenko, and M. Ovchinnikov, *Constraints from the CHARM experiment on Heavy Neutral Leptons with tau mixing*, [arXiv:2107.14685](#).
- [85] **CHARM** Collaboration, F. Bergsma et al., *A Search for Decays of Heavy Neutrinos*, *Phys. Lett. B* **128** (1983) 361.
- [86] J. Alcaide, S. Banerjee, M. Chala, and A. Titov, *Probes of the Standard Model effective field theory extended with a right-handed neutrino*, *JHEP* **08** (2019) 031, [[arXiv:1905.11375](#)].
- [87] A. Biekötter, M. Chala, and M. Spannowsky, *The effective field theory of low scale see-saw at colliders*, *Eur. Phys. J. C* **80** (2020), no. 8 743, [[arXiv:2007.00673](#)].
- [88] T. Li, X.-D. Ma, and M. A. Schmidt, *General neutrino interactions with sterile neutrinos in light of coherent neutrino-nucleus scattering and meson invisible decays*, *JHEP* **07** (2020) 152, [[arXiv:2005.01543](#)].
- [89] T. Li, X.-D. Ma, and M. A. Schmidt, *Constraints on the charged currents in general neutrino interactions with sterile neutrinos*, [arXiv:2007.15408](#).
- [90] R. Mandal, C. Murgui, A. Peñuelas, and A. Pich, *The role of right-handed neutrinos in $b \rightarrow c\tau\bar{\nu}$ anomalies*, *JHEP* **08** (2020), no. 08 022, [[arXiv:2004.06726](#)].
- [91] **COHERENT** Collaboration, D. Akimov et al., *Observation of Coherent Elastic Neutrino-Nucleus Scattering*, *Science* **357** (2017), no. 6356 1123–1126, [[arXiv:1708.01294](#)].
- [92] T. Han, J. Liao, H. Liu, and D. Marfatia, *Scalar and tensor neutrino interactions*, *JHEP* **07** (2020) 207, [[arXiv:2004.13869](#)].
- [93] I. Bischer and W. Rodejohann, *General neutrino interactions from an effective field theory perspective*, *Nucl. Phys. B* **947** (2019) 114746, [[arXiv:1905.08699](#)].
- [94] J. L. Rosner, S. Stone, and R. S. Van de Water, *Leptonic Decays of Charged Pseudoscalar Mesons - 2015*, [arXiv:1509.02220](#).
- [95] H. K. Dreiner, M. Kramer, and B. O’Leary, *Bounds on R -parity violating supersymmetric couplings from leptonic and semi-leptonic meson decays*, *Phys. Rev.* **D75** (2007) 114016, [[hep-ph/0612278](#)].
- [96] D. Ebert, R. Faustov, and V. Galkin, *Relativistic treatment of the decay constants of light and heavy mesons*, *Phys. Lett. B* **635** (2006) 93–99, [[hep-ph/0602110](#)].
- [97] P. Coloma, E. Fernández-Martínez, M. González-López, J. Hernández-García, and Z. Pavlovic, *GeV-scale neutrinos: interactions with mesons and DUNE sensitivity*, *Eur. Phys. J. C* **81** (2021), no. 1 78, [[arXiv:2007.03701](#)].
- [98] R. Escribano, S. González-Solís, P. Masjuan, and P. Sanchez-Puertas, *η' transition form factor from space- and timelike experimental data*, *Phys. Rev. D* **94** (2016), no. 5 054033, [[arXiv:1512.07520](#)].

- [99] X.-W. Gu, C.-G. Duan, and Z.-H. Guo, *Updated study of the η - η' mixing and the thermal properties of light pseudoscalar mesons at low temperatures*, *Phys. Rev. D* **98** (2018), no. 3 034007, [[arXiv:1803.07284](#)].
- [100] Y.-H. Chen, Z.-H. Guo, and B.-S. Zou, *Unified study of $J/\psi \rightarrow PV$, $P\gamma^{(*)}$ and light hadron radiative processes*, *Phys. Rev. D* **91** (2015) 014010, [[arXiv:1411.1159](#)].
- [101] V. Shtabovenko, R. Mertig, and F. Orellana, *FeynCalc 9.3: New features and improvements*, *Comput. Phys. Commun.* **256** (2020) 107478, [[arXiv:2001.04407](#)].
- [102] V. Shtabovenko, R. Mertig, and F. Orellana, *New Developments in FeynCalc 9.0*, *Comput. Phys. Commun.* **207** (2016) 432–444, [[arXiv:1601.01167](#)].
- [103] R. Mertig, M. Bohm, and A. Denner, *FEYN CALC: Computer algebraic calculation of Feynman amplitudes*, *Comput. Phys. Commun.* **64** (1991) 345–359.